PHYSICALLY BASED METHOD FOR MEASURING SUSPENDED-SEDIMENT CONCENTRATION AND GRAIN SIZE USING MULTI-FREQUENCY ARRAYS OF SINGLE-FREQUENCY ACOUSTIC-DOPPLER PROFILERS

David J. Topping, Research Hydrologist, U.S. Geological Survey, Flagstaff, Arizona, dtopping@usgs.gov; Scott A. Wright, Research Hydrologist, U.S. Geological Survey, Sacramento, California, sawright@usgs.gov; Ronald E. Griffiths, Hydrologist, U.S. Geological Survey, Flagstaff, Arizona, rgriffiths@usgs.gov; and David J. Dean, Hydrologist, U.S. Geological Survey, Flagstaff, Arizona, djdean@usgs.gov

Abstract: As the result of a 12-year program of sediment-transport research and field testing on the Colorado River (6 stations in UT and AZ), Yampa River (2 stations in CO), Little Snake River (1 station in CO), Green River (1 station in CO and 2 stations in UT), and Rio Grande (2 stations in TX), we have developed a physically based method for measuring suspended-sediment concentration and grain size at 15-minute intervals using multi-frequency arrays of acoustic-Doppler profilers. This multi-frequency method is able to achieve much higher accuracies than single-frequency acoustic methods because it allows removal of the influence of changes in grain size on acoustic backscatter. The method proceeds as follows. (1) Acoustic attenuation at each frequency is related to the concentration of silt and clay with a known grain-size distribution in a river cross section using physical samples and theory. (2) The combination of acoustic backscatter and attenuation at each frequency is uniquely related to the concentration of sand (with a known reference grain-size distribution) and the concentration of silt and clay (with a known reference grain-size distribution) in a river cross section using physical samples and theory. (3) Comparison of the suspended-sand concentrations measured at each frequency using this approach then allows theory-based calculation of the median grain size of the suspended sand and final correction of the suspended-sand concentration to compensate for the influence of changing grain size on backscatter. Although this method of measuring suspended-sediment concentration is somewhat less accurate than using conventional samplers in either the EDI or EWI methods, it is much more accurate than estimating suspended-sediment concentrations using calibrated pump measurements or single-frequency acoustics. Though the EDI and EWI methods provide the most accurate measurements of suspended-sediment concentration, these measurements are labor-intensive, expensive, and may be impossible to collect at time intervals less than discharge-independent changes in suspended-sediment concentration can occur (< hours). Therefore, our physically based multi-frequency acoustic method shows promise as a cost-effective, valid approach for calculating suspended-sediment loads in river at a level of accuracy sufficient for many scientific and management purposes.

INTRODUCTION

Suspended-sediment concentration and discharge are poorly correlated in many rivers as a result of hysteresis in concentration and grain size produced by (1) changes in the upstream sediment supply and (2) hysteresis in bed roughness arising from lags between discharge and dune geometry during floods. Accurate sediment loads can be calculated in rivers exhibiting these types of hysteresis only if measurements of suspended-sediment concentration are made at time intervals more closely spaced than the timescales over which suspended-sediment concentration is observed to systematically vary independently of water discharge. Single-frequency acoustics have recently become popular for measuring suspended-sediment concentration at high temporal resolution. However, because acoustic attenuation and backscatter are both affected by changes in both the concentration and grain-size distribution of the suspended sediment, concentration biases exceeding a factor of two are common and concentration biases exceeding an order of magnitude are possible when only one acoustic frequency is used. Herein, we describe an unbiased physically based method for measuring suspended-silt-and-clay and suspended-sand concentration, and suspended-sand median grain size (D_{50}) using multi-frequency arrays of side-looking acoustic-Doppler profilers (ADPs), building on the work of Topping et al. (2004, 2006, 2007) and Wright et al. (2010). Data from and the locations of the study sites in this paper are available at: http://www.gcmrc.gov/discharge_qw_sediment/.

THEORETICAL FRAMEWORK

The initial theoretical development that ultimately led to the ability of using acoustics to measure suspended-sediment concentrations and grain-size distributions occurred during the early to mid 20th century, with much of this work occurring during World War II (Urick, 1975). Among the most important contributions of this early research

were the derivation and formalization of the sonar equations (National Defense Research Committee [NDRC], 1946; Urick, 1962). In our study, the following form of the active-sonar equation from Urick (1975) is used:

$$SL - 2TL + TS = RL + DT \tag{1}$$

where SL is the Source Level, $2TL$ is the 2-way Transmission Loss, TS is the Target Strength, RL is the Reverberation Level, and DT is the Detection Threshold. By standard convention, each of these terms is expressed as 10 times a base-10 logarithmic ratio of acoustic intensity, in units of decibels. Knowing the values of all of the terms in equation 1 is not required to approximately calibrate an ADP to measure suspended-sediment concentration. In many studies, only the values of $2TL$ and RL are used in combined, relative-backscatter form to develop such approximate calibrations (e.g., Thevenot et al., 1992; Gartner, 2004; Wall et al., 2006; Wright et al., 2010; Wood and Teasdale, 2013). These calibrations are referred to as approximate because they hold TS constant and therefore do not take into account how changes in the grain-size distribution of the suspended sediment affect TS. Depending on the instrument frequency and the grain-size distributions in suspension, neglecting the effects of changing grain size on TS can lead to substantial biases in ADP measurements of suspended-sediment concentration. Following the convention of Thevenot et al. [1992], the relative backscatter,

$$B = RL + 2TL \tag{2}$$

thus allowing equation 1 to be rewritten as:

$$SL - DT - B + TS = 0\ . \tag{3}$$

SL of the ADPs used in this study ranges from 191 to 196 dB; DT has been determined in this study to range from ~35 to 50 dB, and is the level associated with zero concentration of suspended sediment in the water. B is calculated for each cell along an acoustic beam where the amplitude of the acoustic signal strength, A, exceeds the effective noise floor. The effective noise floor is the sum of the ADP-measured noise floor and the noise-floor offset (determined by an iterative process that removes dependence of the measured acoustic attenuation and backscatter on cell number). In each cell,

$$RL = k_{\mathrm{SF}} A \tag{4}$$

where A is the amplitude of the acoustic signal strength measured in counts, and k_{SF}=0.43 is a scale factor used to convert counts to decibels. By standard convention (Urick, 1975),

$$2TL = 20\log(r) + 2\alpha_{\mathrm{W}} r + 2\alpha_{\mathrm{S}} r \tag{5}$$

where r is the distance along the beam from the transducer to each cell in meters, 20log(r) is the spherical spreading loss term, α_{W} is the coefficient of absorption for acoustic energy in water in dB/m (depends only on temperature at the shallow-water and low-salinity conditions in rivers), and α_{S} is the sediment attenuation coefficient in dB/m. For convenience in solving for α_{S}, a new term is defined, the fluid-corrected backscatter (Wright et al., 2010),

$$B_{\mathrm{F}} = RL + 20\log(r) + 2\alpha_{\mathrm{W}} r \tag{6}$$

with α_{S} then being determined by least-squares linear regression where the values of B_{F} are regressed on r (Topping et al., 2006, 2007b) while iteratively solving for the effective noise floor. In this regression, α_{S} is equal to -1/2 times the slope of the relation between r and B_{F}. Once α_{S} is known, B is then calculated in each cell where A exceeds the effective noise floor, finally allowing calculation of the beam-averaged backscatter, $\overline{B}$. $\overline{B}$ is B averaged first among all cells in a beam and them among all beams used on an ADP.

Attenuation: Acoustic attenuation caused by the presence of suspended sediment arises from two distinctly different physical processes that vary in importance largely as a function of instrument frequency, sediment grain size, and sediment density (Flammer, 1962). These processes are acoustic attenuation from: viscous losses arising from viscous drag between the water and sediment grains (Urick, 1948), and scattering losses arising from the

scattering of sound by the sediment grains in directions other than back toward the detector (Lamb, 1945; Urick, 1948; Morse, 1948). Viscous losses dominate when the suspended sediment is relatively fine whereas scattering losses dominate when the suspended sediment is relatively coarse. We use the conventions and methods of Urick (1948), Flammer (1962), Hay (1983), and Moore et al. (2013) to calculate a sediment attenuation coefficient (α_S) that includes the effects of both viscous- and scattering-losses as well as the effects of multiple grain sizes and wet densities of sediment. Following Urick (1948), α_S is the product of the unit sediment attenuation coefficient, α_{UNIT}, and the concentration of suspended sediment, C:

$$\alpha_S = \alpha_{UNIT} C \ . \tag{7}$$

In our study, the unit sediment attenuation coefficient is defined as the sediment attenuation coefficient at a suspended-sediment concentration of 1 mg/L, with α_S expressed in units of dB/m and C expressed in units of mg/L. α_{UNIT} is the combined ensemble-averaged viscous and scattering attenuation coefficients and is derived in this study using the equations of Moore et al. (2013), and making the appropriate conversions, such that it is expressed in units of decibel-liter per meter-milligram or dB-L/m-mg. Changes in the sorting and density of the suspended-sediment grain-size distribution and the frequency of the ADP all have a major influence on α_{UNIT} (Figure 1). From the example in Figure 1b, it is evident that there exists an optimal range of acoustic frequency, suspended-sand D_{50}, and suspended-silt-and-clay D_{50} where the sand contributes very little to α_{UNIT} and:

$$\alpha_S \approx \alpha_{UNIT} C_{SILT\text{-}CLAY} \tag{8}$$

where $C_{SILT\text{-}CLAY}$ is the suspended-silt-and-clay concentration. In many rivers the D_{50} of the suspended sand ranges from 0.0625 to ~0.25 mm (very fine to fine sand) and, in the absence of flocculation, the D_{50} of the suspended silt and clay ranges from ~0.0005 to ~0.01 mm (fine clay to fine silt). For the sorting of the grain-size distributions portrayed in Figure 1b, these median grain sizes result in a fair degree of separation between the value of α_{UNIT}

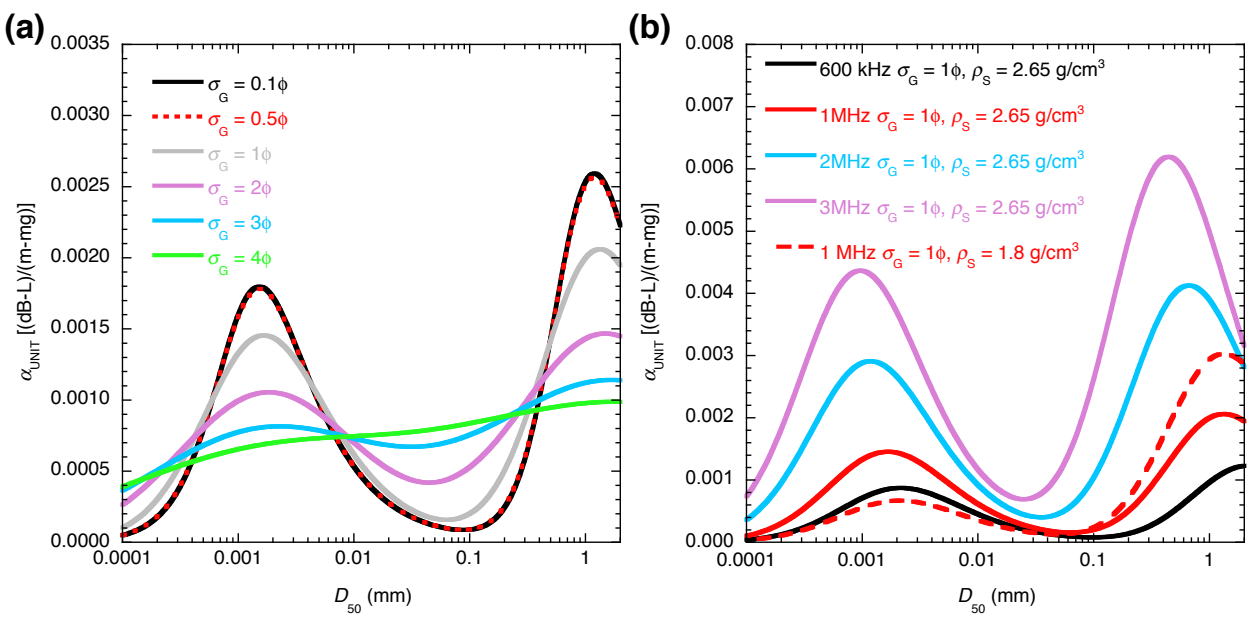

Figure 1 Effects of changes in (a) sediment sorting and (b) ADP frequency and sediment density (ρ_S) on α_{UNIT}. (a) Predicted values of α_{UNIT} at the 1-MHz frequency for the D_{50} of log-normal suspended-sediment grain-size distributions with geometric standard deviations (σ_G) of 0.1ϕ, 0.5ϕ, 1ϕ, 2ϕ, 3ϕ, and 4ϕ. ρ_S is held constant at 2.65 g/cm^3 (quartz density) in this example. (b) Predicted values of α_{UNIT} at acoustic frequencies of 600 kHz, 1 MHz, 2 MHz, and 3 MHz for the D_{50} of log-normal suspended-sediment grain size distributions with σ_G = 1ϕ and ρ_S = 2.65 g/cm^3, and α_{UNIT} at 1 MHz for the D_{50} of log-normal suspended-sediment grain size distributions with σ_G = 1ϕ and a montmorillonite wet ρ_S = 1.8 g/cm^3.

associated with the sand and the value of α_{UNIT} associated with the silt and clay, especially at lower acoustic frequencies. For these median grain sizes and acoustic frequencies, and so long as the suspended-sand concentration does not greatly exceed $C_{\mathrm{SILT\text{-}CLAY}}$, $C_{\mathrm{SILT\text{-}CLAY}}$ can therefore be reasonably accurately predicted by α_{S}. This result allowed Topping et al. (2006, 2007) and Wright et al. (2010) to develop their first-cut single-frequency approximate method of using acoustic attenuation to measure suspended-silt-and-clay concentration and acoustic backscatter to measure suspended-sand concentration.

Target strength and backscatter: Target strength, *TS*, is determined by the amount and nature of the sediment in suspension and by the dimensions of the ensonified volume (NDRC, 1946; Urick, 1975). Much research has been completed on the acoustic scattering effects of individual and, later, concentrations of particles in suspension (Rayleigh, 1896; NDRC, 1946; Urick, 1975; Sheng and Hay, 1988; Hay, 1991; Hay and Sheng, 1992; Thorne and Campbell, 1992; He and Hay, 1993; Thorne et al., 1993, 1995; Thorne and Hanes, 2002; Thorne and Buckingham, 2004; Thorne and Meral, 2008; Moore and Hay, 2009). Although the initial work in this field was conducted on regularly shaped particles, sufficient work using natural sand grains (in both single and mixtures of grain sizes) has allowed a sufficiently robust theory on how sound is backscattered by suspensions of sediment in water. The equation used to derive the relation for *TS* is the following version of the Thorne et al. (1993) equation:

$$P_{\mathrm{rms}} = P_0 r_0 f \left[\frac{3Mtc}{8D\rho_{\mathrm{S}}} \right]^{1/2} \frac{0.96}{ka_{\mathrm{T}}\psi r} \mathrm{e}^{(-2\alpha_{\mathrm{N}} r)} \tag{9}$$

where P_{rms} is the reverberation-level pressure measured at the transducer (in Pascals), P_0 is the source-level pressure (in Pascals) at distance r_0 = 1 m from the transducer, r is the distance along the beam from the transducer (in meters), f is the nondimensional form function that describes the backscattering strength of sediment grains in water as a function of ka_{S}, $k = 2\pi/\lambda$ is the wave number (in 1/m), λ is the acoustic wavelength (in meters), a_{S} is the radius of the sediment grains (in meters), D is the diameter of the sediment grains (in meters), ρ_{S} is the density of sediment (in kg/m^3), M is the mass concentration of suspended sediment (in kg/m^3), t is the acoustic pulse duration (in seconds), c is the measured speed of sound (in m/s), a_{T} is the radius of the transducer (in meters), α_{N} is the attenuation coefficient (in nepers/m) resulting from the sum of α_{W} and α_{S}, and ψ is the non-dimensional near-field correction of Downing et al. (1995) that accounts for non-spherical spreading losses very near the transducer. We exclude this near-field correction because it is either negligible or, at higher frequencies, degrades the results by overcorrecting B_{F} in the first cell, thus resulting in negative biases in α_{S} that get larger with increasing $C_{\mathrm{SILT\text{-}CLAY}}$.

The form function, f, used in this study is that of Thorne and Meral (2008), which takes into account both the effect of the non-spherical shape of natural sediment grains and the effect of multiple grain sizes. Relative to form functions evaluated for single-size spheres, these two effects combine to result in a substantial increase in f in the Rayleigh scattering regime ($ka_{\mathrm{S}} < 1$), and a smaller decrease in the geometric scattering regime. Because this form function is used, M in equation 9 is the concentration of the grain-size distribution of suspended sediment with median grain size D_{50}. Hence, D in equation 9 is replaced with D_{50}. The fact that f and D_{50} are associated with a grain-size distribution and not just a single sediment grain size has major implications with respect to the derivation and physical interpretation of the target strength. The target strength derived below is therefore that for the entire grain-size distribution of sediment in suspension and not that for only sand. In cases where the amount of silt and clay greatly exceeds the amount of sand in suspension, the target strength will approach that for the suspended-silt-and-clay grain-size distribution and will be much different from the target strength for the suspended-sand grain-size distribution. One of the greatest source of error/bias in the methods used in previous studies that have related acoustic backscatter to the concentration of only suspended sand arises from these studies neglecting this important physical effect.

Because acoustic intensity is acoustic pressure squared and 1 neper = 8.686 dB, following the appropriate substitutions, simplifications, and rearrangement, equation 9 can be rewritten in the following decibel form:

$$RL = SL + \left[-20\log(r) - 2\log\alpha_{\mathrm{W}} r - 2\log\alpha_{\mathrm{S}} r \right] + 10\log\left[f^2 \frac{3Mtc}{8D_{50}\rho_{\mathrm{S}}} \left(\frac{0.96}{ka_{\mathrm{T}}} \right)^2 \right] \tag{10}$$

to be consistent with equation 1 and then further simplified to:

$$SL - B + 10\log\left[f^2 \frac{3Mtc}{8D_{50}\rho_S}\left(\frac{0.96}{ka_T}\right)^2 \right] = 0 \,. \tag{11}$$

Simple comparison of equation 3 and equation 11 suggests incorrectly that the right term of the three terms in equation 11 is essentially the target strength minus the detection threshold. Closer inspection of these two equations, however, indicates a problem arising from the conversion of equation 9 from pressure form to the logarithmic intensity form in equation 10 compatible with the sonar equations. When M goes to zero in equation 9, the reverberation-level pressure, P_{rms} also goes to zero. However, when M goes to zero in equation 11, RL goes to minus infinity, because the logarithm of zero is an infinitely large negative number. This problem can be corrected by limiting solution of equation 11 to only those cases where $M > 0$ and by adding a new term from equation 3, the detection threshold, DT. As used in this study, DT is slightly lower than the lowest measured RL in this study during conditions when the suspended-sand concentration was immeasurably small (<0.01 mg/L), conditions when RL is typically less than ~40 to 50 dB. Thus equation 11 can be written in final form as:

$$SL - DT - B = -TS = -10\log\left[f^2 \frac{3Mtc}{8D_{50}\rho_S}\left(\frac{0.96}{ka_T}\right)^2 \right] \tag{12}$$

and can be solved only when $M > 0$.

To finish the derivation of TS such that it is compatible with the backscatter – sediment-concentration relations derived from the sonar equations for constant grain size by Thevenot and others (1992), we: (1) convert M from SI units into the more conventional sediment-concentration units of mg/L and convert D_{50} from SI units into the more appropriate units of mm for sand and finer sediment (these two conversions cancel each other out), and (2) break TS in equation 12 into two parts, the Unit Target Strength, UTS, and, C, the concentration in mg/L of suspended sediment in a log-normal grain-size distribution with median grain size D_{50}. In this two-part form,

$$TS = UTS + 10\log C \tag{13}$$

where,

$$UTS = 10\log\left[f^2 \frac{3tc}{8D_{50}\rho_S}\left(\frac{0.96}{ka_T}\right)^2 \right] \tag{14}$$

and $UTS = TS$ when $C = 1$ mg/L. By virtue of equation 13 a tenfold change in C will result in a 10 dB change in TS when the grain-size distribution of the suspended sediment remains constant. Changes in the grain-size distribution affect both f and D_{50} in equation 13, resulting in a more complicated influence on TS than do changes in C.

The more complicated influence on TS of changes in the sand grain-size distribution under constant C is best illustrated through calculation of the Relative Unit Target Strength ($RUTS$), that is, the UTS relative to the UTS associated with a reference D_{50}, denoted as $D_{50\text{-REF}}$. $D_{50\text{-REF}}$ is the median grain size at a given location that best characterizes the D_{50} of the suspended sediment over the widest possible range in concentration. For convenience, the UTS associated with $D_{50\text{-REF}}$ is abbreviated as UTS_{REF}. $RUTS$ is calculated by simply subtracting UTS_{REF} from the UTS for all values of D_{50}. By virtue of the behavior of the $RUTS$, backscatter measurements made with higher-frequency ADPs are generally less sensitive to changes in suspended-sand D_{50} than are backscatter measurements made with lower-frequency ADPs. The $RUTS$ increases rapidly as a function of increasing D_{50} over most of the Rayleigh scattering regime, and only begins to plateau around ka_S ~0.5. The main implication of this result is that, when $ka_S < 0.5$, use of a single-frequency acoustic approach to measure suspended-sand concentration will be highly biased as a result of concentration-independent variation in D_{50}. Comparison between measured and theoretically determined values of the $RUTS$ are good (Figure 2). The behavior of the $RUTS$ as a function of frequency and D_{50} is

the physical process that allows accurate, that is, relatively unbiased, backscatter-based measurements of suspended-sand concentration and D_{50} to be possible when multiple acoustic frequencies are used.

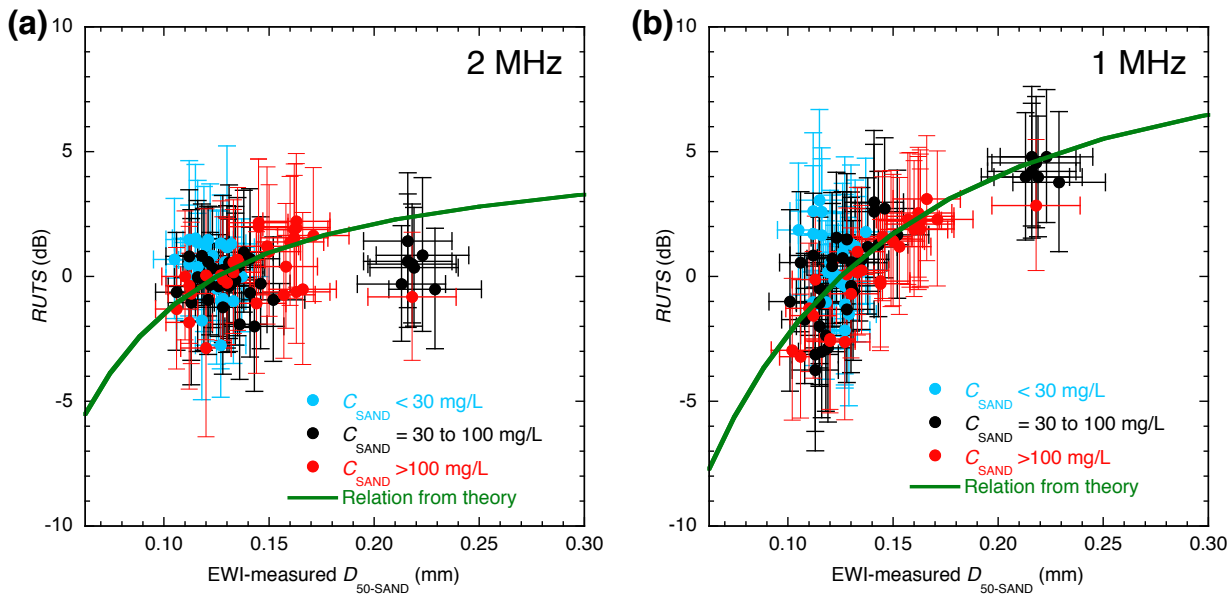

Figure 2 Comparisons of measured and theoretical values of *RUTS* at the Colorado River near river mile 30, 09383050, (CR30) study site, at (a) 2-MHz and (b) 1-MHz acoustic frequencies. Measured values of the *RUTS* are segregated into three different concentration ranges in these plots to allow evaluation of whether they depend on concentration; as indicated in these plots, there is no discernable dependence of the measured *RUTS* on concentration. $D_{50\text{-SAND}}$ error bars are 95%-confidence-level error bars that include both field and laboratory-processing errors in the EWI measurements of $D_{50\text{-SAND}}$; *RUTS* error bars are 95%-confidence-level error bars that include (1) both field and laboratory-processing errors in the EWI measurements of C_{SAND}, (2) a 2% estimated error in the ADP-calculated values of $\overline{B}$, and (3) the 95%-confidence-level error in the mean value of $\overline{B}$ time-averaged over the 1-hour interval centered on the temporal midpoint of the time of each EWI measurement.

Our derivation of the *UTS* and *RUTS* allows the Thevenot et al. (1992) simplification of the sonar equation to be re-derived in a convenient form for cases of varying grain size; a form that in this study uses backscatter measured at multiple frequencies to solve for both suspended-sediment concentration and D_{50}. In their simplification of the active sonar equation, Thevenot et al. (1992) showed that, when grain size is constant:

$$C = 10^{-0.1K+0.1B} \tag{15}$$

where C is sediment concentration in mg/L, B is relative backscatter (replaced in this study by $\overline{B}$ the beam-averaged backscatter), and K is a constant. Substituting equations 13 and 14 into equation 12 and rearranging equation 12 to be in the form of Thevenot et al. [1992] indicates that, when grain-size is allowed to vary, K is not truly constant, but is the sum of a constant part ($SL - DT$) and a varying part (UTS). The rearranged version of equation 12 after these substitutions is:

$$C = 10^{-0.1(SL-DT+UTS)+0.1\overline{B}} . \tag{16}$$

Thus, a generalized way to re-derive equation 15 such that grain size is free to vary is to define a new constant:

$$K_1 = SL - DT \tag{17}$$

and rewrite equation 16 as:

$$C = 10^{-0.1K_1 - 0.1UTS + 0.1\overline{B}} . \tag{18}$$

For the special case, where C is the concentration of suspended sediment with D_{50} equal to $D_{50\text{-REF}}$,

$$C = 10^{-0.1K_1 - 0.1UTS_{\text{REF}} + 0.1\overline{B}} . \tag{29}$$

Because

$$RUTS = UTS - UTS_{\text{REF}} \tag{20}$$

the general case where the median grain size of the sediment in suspension is allowed to vary can be written as:

$$C = 10^{-0.1K_1 - 0.1UTS_{\text{REF}} - 0.1RUTS + 0.1\overline{B}} . \tag{21}$$

Because UTS_{REF} is constant at a given study site, it is convenient to define another new constant:

$$K_2 = -\left(K_1 + UTS_{\text{REF}}\right) = -0.1\left(SL - DT + UTS_{\text{REF}}\right) \tag{22}$$

allowing the final more-general form of equation 15 for varying grain size:

$$C = 10^{K_2 + 0.1\left(\overline{B} - RUTS\right)} . \tag{23}$$

If only one frequency ADP is present, it is theoretically impossible to solve for both C and $RUTS$ for a given measured $\overline{B}$. However, if two or more frequencies are present, it is possible to iteratively solve for C and $RUTS$. This iterative approach is the basis for the method we use to calculate suspended-sand C and D_{50}.

As a grain-size distribution of suspended sediment broadens, the difference in the UTS between silt-and-clay- and sand-size sediment lessens as a result of the effect of decreased sorting on the form function. In cases where the geometric standard devation, σ_G, of a grain-size distribution is less than ~1.5ϕ, the UTS associated with silt grain-size distributions will be much less than the UTS associated with sand grain-size distributions. In these cases, the backscatter will be dominantly produced by sand-size sediment. Conversely, in cases where the σ_G of a grain-size distribution exceeds ~1.5ϕ, the UTS associated with silt grain-size distributions becomes a larger fraction of the UTS associated with sand grain-size distributions, and measurable backscatter will be produced by the silt-size sediment in addition to the backscatter produced by the sand-size sediment. Ultimately, in cases where the σ_G of a grain-size distribution exceeds ~3ϕ, the UTS associated with grain-size distributions of silt and clay will be nearly equal to the UTS associated with grain-size distributions of sand. Under these conditions, the backscatter produced by the suspended silt and clay is nearly as much as that produced by the suspended sand. Because the sorting of suspended silt and clay (σ_G = 2 to 3ϕ) is much broader than the sorting of suspended sand (σ_G = 0.63 to 0.65ϕ) at our study sites, a condition likely in most rivers, the backscatter produced by silt and clay must be accounted for under conditions when the concentration of the suspended silt and clay greatly exceeds that of the sand.

To allow accurate acoustic measurements of suspended-sand concentration to be made when even large concentrations of silt and clay are present (and most of $\overline{B}$ arises from the amount of silt and clay in suspension), a data-processing method was developed to allow separation of the part of $\overline{B}$ arising from sand-size sediment from the part of $\overline{B}$ arising from silt-and-clay-sized sediment. This method utilizes the differing theoretical behaviors of the UTS and α_S under different combinations of suspended silt and clay and suspended sand. An early empirical version of this method was described in Topping et al. (2007). The basis for the UTS part of this method is the development of a Base-Backscatter-Calibration (BBC) relation between $\overline{B}$ and the log-transformed EDI/EWI-measured suspended-sand concentration using equation 23 for conditions where the suspended sediment is

dominated by sand-size sediment with a median grain size within ¼ϕ of $D_{50\text{-REF}}$ and assumed constant sorting. Relations are then developed using both theory and empirical analysis to account and correct for the excess backscatter relative to this relation for conditions where the amount of silt and clay greatly exceeds the amount of sand in suspension. For accurate BBC relations to be developed, the average concentration of suspended sand along the beam must systematically relate to the EDI/EWI-measured velocity-weighted concentration of suspended sand in the cross section. Because of how the flow and suspended-sediment-concentration field interact with the local channel geometry at the locations of ADP deployments, there are typically differences between the average suspended-sand C and D_{50} in the part of the cross section ensonified by the ADP beams and the velocity-weighted suspended-sand C and D_{50} in entire EDI/EWI cross section. These differences lead to differences between the theoretically predicted (0.1 by equation 23) and empirically determined slopes and y-intercepts of the BBC relations. The BBC relation form of equation 23 allowing empirically determined slopes and y-intercepts is:

$$\log\left(C_{\text{SAND-REF}}\right) = K_2 + K_3\overline{B}_{\text{BASE}} \tag{24}$$

where $C_{\text{SAND-REF}}$ is the EDI/EWI-measured reference concentration in the river cross section of suspended sand with a median grain size equal to $D_{50\text{-REF}}$, and $\overline{B}_{\text{BASE}}$ is the base backscatter associated with $C_{\text{SAND-REF}}$.

The additional beam-averaged backscatter required to account for the amount of backscatter produced by the presence of suspended silt and clay at a given concentration of suspended sand is referred to as the excess backscatter, B'. Excess backscatter is calculated as:

$$B' = \overline{B} - \overline{B}_{\text{BASE}} \,. \tag{25}$$

Because

$$\overline{B} = TS + SL + DT \tag{26}$$

equation 25 can be rewritten as:

$$B' = \left(TS_{\text{SED}} + SL + DT\right) - \left(TS_{\text{SAND-REF}} + SL + DT\right) \tag{27}$$

and simplified to:

$$B' = TS_{\text{SED}} - TS_{\text{SAND-REF}} \,, \tag{28}$$

where TS_{SED} is the target strength of the suspended sand, silt, and clay mixture and $TS_{\text{SAND-REF}}$ is the target strength of $C_{\text{SAND-REF}}$. By definition, when all of the suspended sediment is composed of sand with $D_{50} = D_{50\text{-REF}}$, $B' = 0$. To derive the theoretically based value of B' at constant sand concentration and D_{50}, equation 13 can be rewritten as:

$$TS = 10\log\left[\frac{f^2}{D_{50}\rho_{\text{S}}}\right] + 10\log C + 10\log\left[\frac{3tc}{8}\left(\frac{0.96}{ka_{\text{T}}}\right)^2\right]. \tag{29}$$

After rearrangement and substitution of the quartz density of 2.65 g/cm^3 for the density of sand and replacement of the 0.1 theoretical slope of the BBC relation with the empirical slope K_3, equation 29 becomes:

$$B' = \left(\frac{1}{K_3}\right)\log\left[\left(\frac{f_{\text{SED}}}{f_{\text{REF}}}\right)^2\left(\frac{D_{50\text{-REF}}}{D_{50\text{-SED}}}\right)\left(\frac{2.65}{\rho_{\text{SED}}}\right)\left(1 + \frac{C_{\text{SILT-CLAY}}}{C_{\text{SAND-REF}}}\right)\right] \tag{30}$$

where $C_{\text{SILT-CLAY}}$ is the concentration of silt and clay in mg/L, $D_{50\text{-SED}}$ is the median grain size of the sand, silt, and clay mixture in suspension, f_{SED} is the value of the Thorne and Meral (2008) form function calculated for the grain-size distribution of the sand, silt, and clay mixture, ρ_{SED} is the wet density of the sand, silt, and clay mixture, and f_{REF}

is the value of the Thorne and Meral (2008) form function associated with the $D_{50\text{-REF}}$ of the suspended sand. The theoretical behavior of B' predicted by equation 30 agrees well with the empirical behavior of B' (Figure 3).

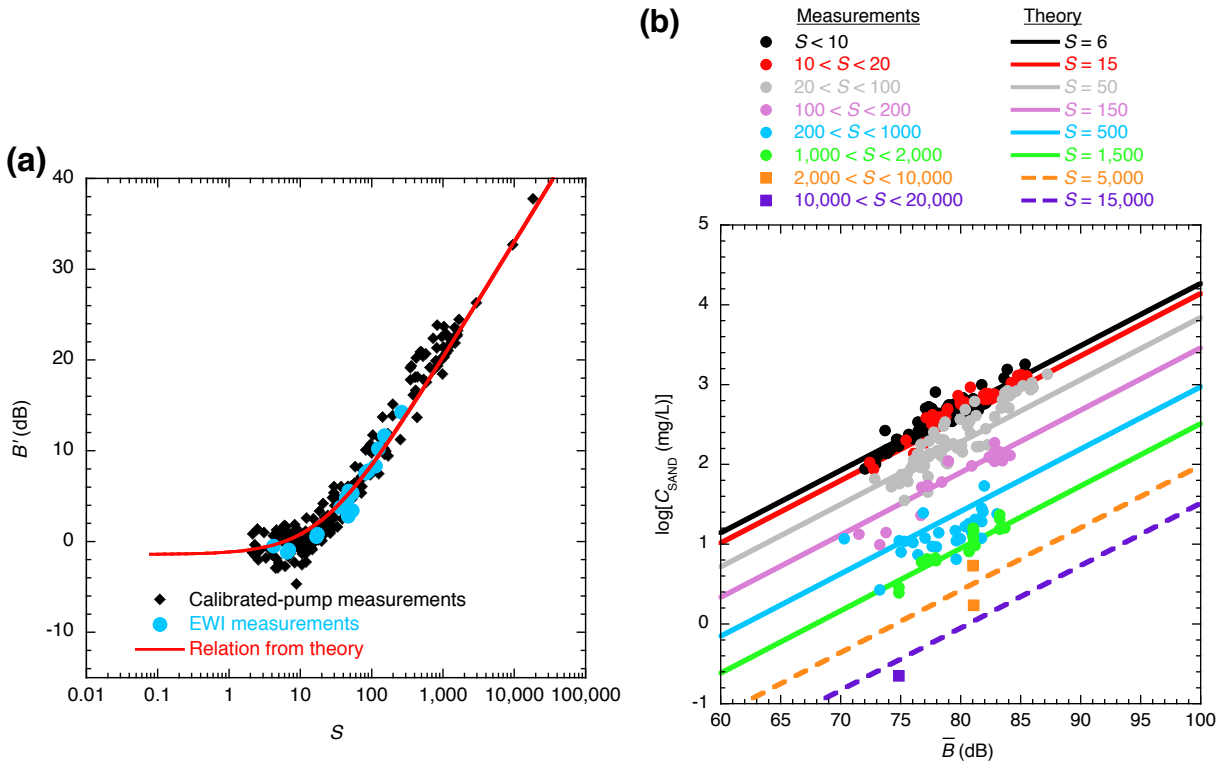

Figure 3 (a) B' plotted as a function of S for the 2-MHz ADP at the Rio Grande above Rio Grande Village, TX, 08375295, (RG-RGV) study site. The BBC relation used to calculate values of B' has a slope of 0.078. The theoretical relation for B' is derived using a sand grain-size distribution with $D_{50\text{-REF}}$ = 0.105 mm and $\sigma_G = 0.65\phi$, and a silt and clay grain-size distribution with D_{50} = 0.002 mm, $\sigma_G = 2.7\phi$, and a wet density of 2.65 g/cm^3. (b) Log(C_{SAND}) plotted as a function of $\overline{B}$ for 8 different ranges of S for the 2-MHz ADP at the RG-RGV study site. Measurements plotted are the same as in a. BBC relation fit to suspended-sediment measurements with $S \leq 10$ shown as solid black line; theoretical relations between $\overline{B}$ and log(C_{SAND}) at higher values of S calculated using the theoretical B' relation in a.

As a result of the theoretical behaviors of backscatter and attenuation under different suspended-sediment grain-size distributions, the backscatter produced by extremely high concentrations of suspended silt and clay can effectively mask the backscatter produced by sand when the ratio of suspended silt and clay to suspended sand, S, is high. As a result of backscatter masking by relatively high concentrations of suspended silt and clay, theoretically derived relations between $\overline{B}$ and log(C_{SAND}) at constant α_S become extremely steep (with almost no slope) at lower values of log(C_{SAND}), making it problematic to accurately solve for log(C_{SAND}). The steepness transition in these relations occurs at increasing values of S as the D_{50} of the silt and clay decreases. To calculate C_{SAND} using only the backscatter produced by the suspended sand, we subtract the silt-and-clay produced excess backscatter B' from measurements of $\overline{B}$ by using theoretically derived relations between $\overline{B}$, α_S, log(C_{SAND}), and S calculated on the basis of equations 8, 24, and 30 (Figure 4).

TWO-FREQUENCY *RUTS* METHOD

The two-frequency *RUTS* method for measuring C_{SAND} and D_{50} is an iterative process that uses as input (1) the single-frequency 1- and 2-MHz estimates of C_{SAND} calculated using the theory described in the previous section and (2) the theoretical relations between suspended-sand D_{50} and the *RUTS* at the 1- and 2-MHz frequencies. Because backscatter at higher frequencies is less affected by changes in the D_{50} of the suspended sand, the 2-MHz

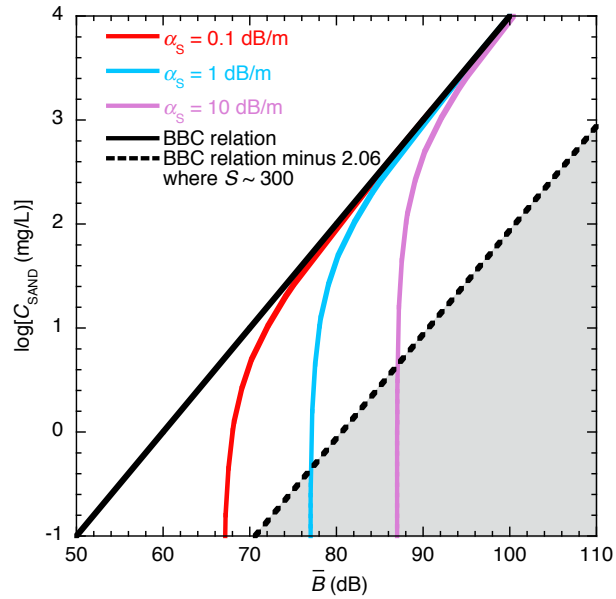

Figure 4 Behavior of theoretical relations between $\bar{B}$ and log(C_{SAND}) for different values of α_S at the 1-MHz frequency. The gray shaded regions indicate the regions of backscatter masking produced by relatively high concentrations of suspended silt and clay. Suspended-sand D_{50} = 0.125 mm, $\sigma_G = 0.63\phi$; suspended-silt-and-clay D_{50} = 0.001 mm, $\sigma_G = 3\phi$, ρ_S = 2.65 g/cm^3. BBC relation has a slope (K_3) of 0.1 and a y-intercept (K_2) of -6. Shown are the BBC relation and the relations between $\bar{B}$ and log(C_{SAND}) for the cases where α_S = 0.1, 1.0, and 10 dB/m. These relations between $\bar{B}$ and log(C_{SAND}) are near vertical when S exceeds ~300 in the gray shaded region.

estimate of C_{SAND} is chosen as the initial concentration estimate in this calculation. The difference in the values of $\bar{B}$ measured at the 1- and 2-MHz frequencies (corrected for B'), the theoretical *RUTS* relations, and the BBC relations for the 1- and 2-MHz ADPs are then used in an iterative fashion to calculate the D_{50} and concentration of the suspended sand that satisfies the constraint that the B'-corrected values of $\bar{B}$ measured at each frequency are associated with the same suspended-sand concentration. By this process, when the 1-MHz estimate of C_{SAND} exceeds the 2-MHz estimate, the suspended-sand D_{50} is calculated to be greater than $D_{50\text{-REF}}$ using the 1-MHz *RUTS* relation and the two-frequency value of C_{SAND} is calculated to be lower than the initial 2-MHz estimate of C_{SAND} using the 2-MHz *RUTS* relation and this new value of D_{50}. Conversely, when the 1-MHz estimate of C_{SAND} is lower than the 2-MHz estimate of C_{SAND}, the suspended-sand D_{50} is calculated to be less than $D_{50\text{-REF}}$ using the 1-MHz *RUTS* relation and the two-frequency value of C_{SAND} is calculated to be higher than the initial 2-MHz estimate of C_{SAND} using the 2-MHz *RUTS* relation and this new value of D_{50}. Compared to the initial single-frequency estimates of C_{SAND}, two-frequency measurements of C_{SAND} by this process are generally unbiased as a function of changing suspended-sand D_{50} (Figure 5). As expected on the basis of the theoretical behavior of the *RUTS* depicted in Figure 2, grain-size-driven biases in 1-MHz estimates of C_{SAND} are greater than in 2-MHz estimates of C_{SAND}.

RESULTS

Unless the range in suspended-sand D_{50} at a study site is smaller than about 1ϕ, two acoustic frequencies are required to produce measurements of suspended-sand concentration (C_{SAND}) that are unbiased by changes in the suspended-sand grain-size distribution. In cases where the range in suspended-sand D_{50} is smaller than about 0.75ϕ, reasonably unbiased results may be obtained by using only a single 2-MHz-frequency ADP, but only if the contribution of silt and clay to backscatter is accounted for. At our study sites, use of a single 1-MHz frequency ADP resulted in biased measurements of C_{SAND} regardless of the range in suspended-sand D_{50}. At almost all of our study sites, inclusion of B' resulted in a substantial reduction in the relative bias in the measurements of C_{SAND}. Furthermore, the inclusion of B' results in a much more substantial reduction in the maximum relative error. For

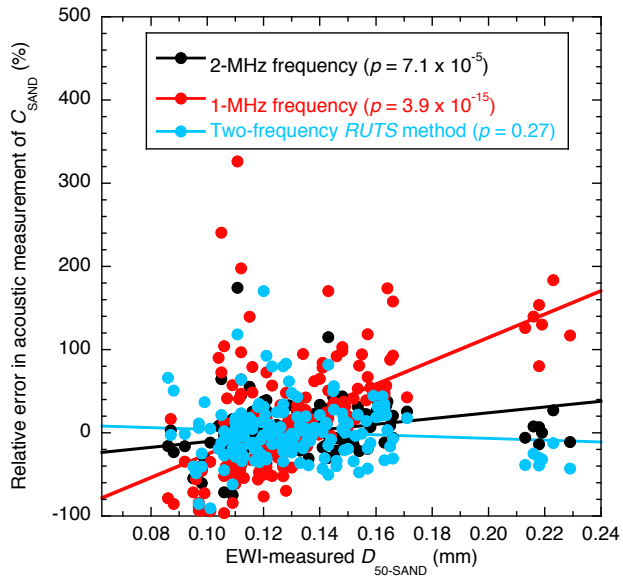

Figure 5 Relative errors in single-frequency and two-frequency acoustic measurements of C_{SAND} at the CR30 study site. F-tests conducted on the least-squares linear regressions fit to these relative errors indicate significant positive correlations (at the p = 0.05 critical level) between suspended-sand D_{50} and error for both the 1- and 2-MHz single-frequency measurements of C_{SAND}, but no significant correlation between suspended-sand D_{50} and error for the two-frequency measurements. The significant relation between suspended-sand D_{50} and error is much steeper at the 1-MHz frequency than at the 2-MHz frequency. These results indicate the presence of grain-size-driven bias in the single-frequency measurements of C_{SAND} that is larger at the lower frequency, as expected on the basis of the theoretical behavior of the *RUTS* depicted in Figure 2.

example, at the RG-RGV study site, the maximum relative error in the acoustic measurements of C_{SAND} when using the single-frequency method at 1 MHz neglecting B' is +95,900%; this enormous relative error decreases to +651% upon inclusion of the effects of B'. Furthermore, among the 173 paired acoustic and EWI measurements at the Colorado River near Grand Canyon, AZ, 09402500, study site, the maximum relative error in the acoustic measurements of C_{SAND} when using the single-frequency method at 2 MHz neglecting B' is +1,410%; this extremely large relative error decreases to +65.6% upon inclusion of the effects of B'.

The two-frequency acoustic measurements compare well with the physical measurements of the velocity-weighted suspended-silt-and-clay, suspended-sand concentrations, and suspended-sand median grain sizes in the river cross sections at the study sites on the Colorado River and Rio Grande (Figure 6). Wilcoxon-Mann-Whitney tests conducted on in- and out-of-sample data from the Colorado River study sites indicate that the in-sample and out-of-sample errors in the acoustic measurements of silt and clay concentration and sand concentration are not significantly different at the 0.05 critical level. In Figure 6a, the acoustic and physical measurements of suspended-silt-and-clay concentration are in good agreement over the range from ~100 mg/L to ~20,000 mg/L; in figure 6b, the acoustic and physical measurements of suspended-sand concentration are in good agreement over the range from ~2 mg/L to ~5,000 mg/L. Though not shown in figure 6a because the physical measurements are calibrated-pump measurements, acoustic and calibrated-pump measurements of suspended-silt-and-clay concentration have been found to agree well at concentrations as high as ~30,000 mg/L on both the Colorado River and Rio Grande. In Figure 6c, the acoustic and physical measurements of suspended-sand D_{50} are in reasonable agreement over the range from ~0.08 to 0.25 mm. Although the variance about the line of perfect agreement in Figure 6c appears larger than in Figures 6a-b, this is a visual artifact of the differences in scale between the figure panels; five orders of magnitude are plotted in Figures 6a-b, whereas less than one order of magnitude is plotted in Figure 6c. In reality, the variance about the line of perfect agreement in Figure 6c is smaller than in Figures 6a-b.

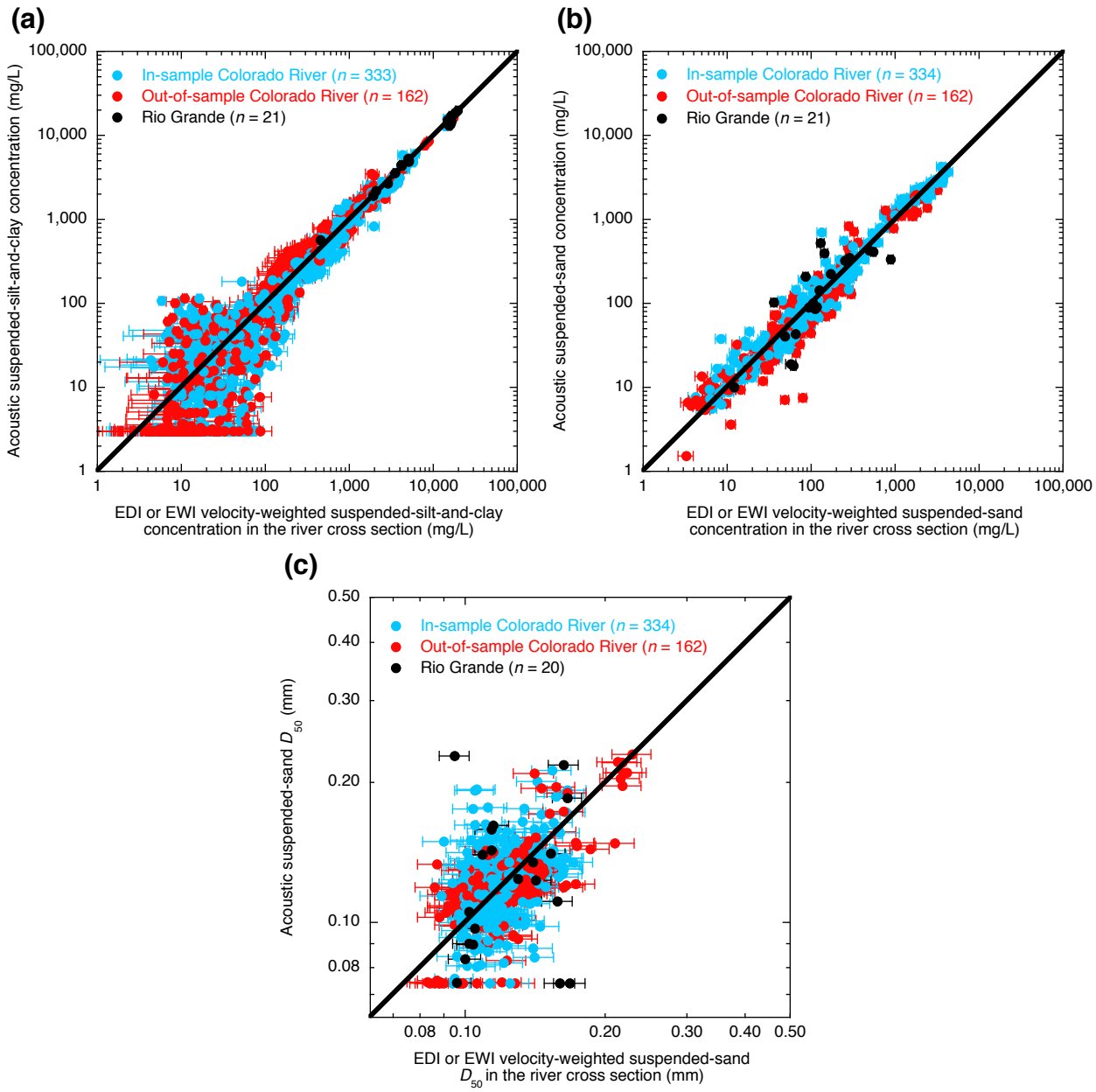

Figure 6 Two-frequency acoustic measurements of the velocity-weighted (a) suspended-silt-and-clay concentration, (b) suspended-sand concentration, and (c) suspended-sand D_{50} in the river cross section plotted as a function of the EDI or EWI-measured values of these parameters at the five Colorado River and Rio Grande study sites where the EDI/EWI measurement cross section is located within 200 m of the ADP arrays. Black solid lines are the lines of perfect agreement between the EDI/EWI measurements at the acoustic measurements. In-sample data are those used in the calibration of either of the two ADPs at a study site; out-of-sample data are not used in any calibration. Horizontal error bars indicate the 95%-confidence-level combined field and laboratory errors in the EDI/EWI measurements calculated using the methods in Topping et al. (2010, 2011).

For all three of the parameters plotted in Figure 6, the the log-transformed variance is approximately symmetric about the lines of perfect agreement, indicating the presence of little bias in the method; a result supported by F-tests conducted on the relative errors associated with each acoustic measurement. Only in the case of the acoustic

measurements of the suspended-sand D_{50} do the F-tests indicate the presence of bias; there is a tendency for a small positive bias in the acoustic measurements of suspended-sand D_{50} when $D_{50} < D_{50\text{-REF}}$ and for a small negative bias in these measurements when $D_{50} > D_{50\text{-REF}}$. Although the two-frequency acoustic measurements are generally unbiased, the presence of reasonably large variance about the lines of perfect agreement indicates that these measurements are subject to relatively large random error. For both suspended silt and clay and suspended sand, the log-transformed variance about the lines of perfect agreement decreases significantly with increasing concentration. In the case of sand, this decrease in variance is gradual, whereas in the case of silt and clay, this decrease in variance is rapid between concentrations of 1 and 100 mg/L and more gradual between concentrations of 100 and 20,000 mg/L. These negative correlations between concentration and the log-transformed variance about the lines of perfect agreement indicate that the relative errors in the acoustic measurements of suspended-silt-and-clay concentration and suspended-sand concentration both decrease with increasing concentration. For suspended-sand D_{50}, the log-transformed variance about the line of perfect agreement, and therefore the relative error in the acoustic measurements of suspended-sand D_{50}, is approximately constant across the measured 0.09 to 0.25-mm range.

REFERENCES

Downing, A., Thorne, P.D., and Vincent, C.E. (1995). "Backscattering from a suspension in the near field of a piston transducer," Journal of the Acoustical Society of America, 97(3), pp. 1614-1620, doi: 10.1121/1.412100.

Flammer, G.H. (1962). "Ultrasonic measurement of suspended sediment," U.S. Geological Survey Bulletin 1141-A, 48 pp.

Gartner, J.W. (2004). "Estimating suspended solids concentrations from backscatter intensity measured by acoustic Doppler current profiler in San Francisco Bay, California," Marine Geology, 211, pp. 169-187, doi: 10.1016/j.margeo.2004.07.001.

Hay, A.E. (1983). "On the remote acoustic detection of suspended sediment at long wavelengths," Journal of Geophysical Research, 88(C12), pp. 7525-7542, doi: 10.1029/JC088iC12p07525.

Hay, A.E. (1991). "Sound scattering from a particle-laden, turbulent jet," Journal of the Acoustical Society of America, 90(4), pp. 2055-2074, doi: 10.1121/1.401633.

Hay, A.E., and Sheng, J. (1992), "Vertical profiles of suspended sand concentration and size from multifrequency acoustic backscatter," Journal of Geophysical Research, 97(C10), pp. 15,661-15,677, doi: 10.1029/92JC01240.

He, C., and Hay, A.E. (1993). "Broadband measurements of the acoustic scattering cross section of sand particles in suspension," Journal of the Acoustical Society of America, 94(4), pp. 2247-2254, doi: 10.1121/1.407496.

Lamb, H. (1945), Hydrodynamics, Sixth edition, 738 pp., Dover Publications, New York.

Moore, S.A., and Hay, A.E. (2009). "Angular scattering of sound from solid particles in turbulent suspension," Journal of the Acoustical Society of America, 126(3), pp. 1046-1056, doi: 10.1121/1.3180696.

Moore, S.A., Le Coz, J., Hurther, D. and Paquier, A. (2013). "Using multi-frequency acoustic attenuation to monitor grain size and concentration of suspended sediment in rivers," Journal of the Acoustical Society of America, 133(4), pp. 1959-1970, doi: 10.1121/1.4792645.

Morse, P. M. (1948), Vibration and sound, Second edition, 468 pp., McGraw-Hill Book Co., New York.

National Defense Research Committee (1946), "Principles and applications of underwater sound," Summary Technical Report of Division 6, volume 7, 295 pp., Washington, D.C.

Rayleigh, Baron, Strutt, J.W. (1896). Theory of sound, vol. 2, 504 pp., Macmillan and Co., New York. [Google Books, http://books.google.com/books?id=Zm9LAAAAMAAJ&pg=PR5&source=gbs_selected_pages&cad=3#v=onepage&q&f=false, accessed on March, 13, 2014]

Sheng, J., and Hay, A.E. (1988), "An examination of the spherical scatterer approximation in aqueous suspensions of sand," Journal of the Acoustical Society of America, 83(2), pp. 598-610, doi: 10.1121/1.396153.

Thevenot, M.M., Prickett, T.L. and Kraus, N.C. (1992) "Tylers Beach, Virginia, Dredged material plume monitoring project 27 September to 4 October 1991," U.S. Army Corps of Engineers Dredging Research Program Technical Report DRP-92-7, 204 pp.

Thorne, P.D., and S.C. Campbell (1992), Backscattering by a suspension of spheres, *Journal of the Acoustical Society of America*, *92*(2), 978-986, doi: 10.1121/1.403967.

Thorne, P.D., and M.J. Buckingham (2004), Measurements of scattering by suspensions of irregularly shaped sand particles and comparison with a single parameter modified sphere model, *Journal of the Acoustical Society of America*, *116*(5), 2876-2889, doi: 10.1121/1.1808458.

Thorne, P.D., and Hanes, D.M. (2002). "A review of acoustic measurements of small-scale sediment processes," Continental Shelf Research, 22(4), pp. 603-632, doi: 10.1016/S0278-4343(01)00101-7.

Thorne, P.D., and Meral, R. (2008). "Formulations for the scattering properties of suspended sandy sediments for use in the application of acoustics to sediment transport processes," Continental Shelf Research, 28(2), pp. 309-317, doi: 10.1016/j.csr.2007.08.002.

Thorne, P.D., Hardcastle, P.J., and Soulsby, R.L. (1993). "Analysis of acoustic measurements of suspended sediments," Journal of Geophysical Research, 98(C1), pp. 899-910, doi: 10.1029/92JC01855.

Thorne, P.D., Waters, K.R., and Brudner, T.J. (1995). "Acoustic measurements of scattering by objects of irregular shape," Journal of the Acoustical Society of America, *97*(1), pp. 242-251, doi: 10.1121/1.413109.

Topping, D.J., Melis, T.S., Rubin, D.M., and Wright, S.A. (2004). "High-resolution monitoring of suspended-sediment concentration and grain size in the Colorado River in Grand Canyon using a laser-acoustic system," in Proc. of the 9th International Symposium on River Sedimentation, Yichang, People's Republic of China, 2004, edited by C. Hu and Y. Tan, pp. 2507–2514.

Topping, D.J., Wright, S.A., Melis, T.S., and Rubin, D.M. (2006). "High-resolution monitoring of suspended-sediment concentration and grain size in the Colorado River using laser-diffraction instruments and a three-frequency acoustic system," Proc. of the 8th Federal Interagency Sedimentation Conference, Reno, Nevada, April 2–6, 2006, CD-ROM, ISBN 0-9779007-1-1.

Topping, D.J., Wright, S.A., Melis, T.S., and Rubin, D.M. (2007). "High-resolution measurements of suspended-sediment concentration and grain size in the Colorado River in Grand Canyon using a multi-frequency acoustic system," Proc. of the Tenth International Symposium on River Sedimentation, Moscow, Russia, August 1–4, 2007, pp. 330–339, ISBN 978-5-89575-124-4, 978-5-89575-127-5.

Topping, D.J., Rubin, D.M., Grams, P.E., Griffiths, R.E., Sabol, T.A., Voichick, N., Tusso, R.B., Vanaman, K.M., and McDonald, R.R. (2010). "Sediment transport during three controlled-flood experiments on the Colorado River downstream from Glen Canyon Dam, with implications for eddy-sandbar deposition in Grand Canyon National Park," U.S. Geological Survey Open-File Report, 2010-1128, 111 pp.

Topping, D.J., Rubin, D.M., Wright, S.A., and Melis, T.S. (2011). "Field evaluation of the error arising from inadequate time averaging in the standard use of depth-integrating suspended-sediment samplers," U.S. Geological Survey Professional Paper, 1774, 95 pp.

Urick, R.J. (1948). "The absorption of sound in suspensions of irregular particles," Journal of the Acoustical Society of America, 20(3), pp. 283-289, doi: 10.1121/1.1906373.

Urick, R.J. (1962). "Generalized form of the sonar equations," Journal of the Acoustical Society of America, 34(5), pp. 547-550, doi: 10.1121/1.1918166.

Urick, R.J. (1975). Principles of Underwater Sound for Engineers, 384 pp., McGraw Hill, New York.

Wall, G.R., Nystrom, E. A., and Litten, S. (2006). "Use of an ADCP to compute suspended-sediment discharge in the tidal Hudson River, New York," U.S. Geological Survey Scientific Investigations Report 2006-5055, 26 pp.

Wood, M.S., and Teasdale, G. N. (2013). "Use of surrogate technologies to estimate suspended sediment in the Clearwater River, Idaho and Snake River, Washington, 2008-10," U.S. Geological Survey Scientific Investigations Report 2013-5052, 29 pp.

Wright, S.A., Topping, D.J., and Williams, C.A. (2010). "Discriminating silt-and-clay from suspended-sand in rivers using side-looking acoustic profilers," Proc. of the 2nd Joint Federal Interagency Conference, Las Vegas, Nevada, June 27-July 1, 2010.